Predictions of the interacting boson approximation in a consistent Q framework

D. D. Warner and R. F. Casten
Brookhaven National Laboratory, Upton, New York 11973
(Received 28 April 1983)

The predictions of the interacting boson approximation are studied in the consistent Q formalism in which the same parametrization of the boson quadrupole operator is used in both the Hamiltonian and in the $E2$ operator. In this scheme, wave functions, relative energies of states of the same spin, and all relative $B(E2)$ values depend on only a single parameter, χ_Q, which appears in the internal structure of the operator Q. This feature allows a number of simple results to be obtained, principally through the construction of contour plots of various observables in terms of χ_Q and the boson number N. The entire SU(3)—O(6) region, including both limiting symmetries, can be treated by allowing χ_Q to vary between its respective limiting values for those two symmetries. For deformed nuclei, a number of characteristic features are obtained, involving the predicted decay of the γ band and the energy and decay of the first 0^+ excitation. It is shown that the dominance of the $\beta\rightarrow\gamma$ over $\beta\rightarrow g$ matrix elements and the near equality of $\beta\rightarrow\gamma$ and $\gamma\rightarrow g$ $E2$ matrix elements are inherent features of the model. The automatic inclusion of band mixing in the interacting boson approximation is discussed in terms of the mixing parameter Z_γ and it is shown that the interacting boson approximation reproduces the empirical systematics in Z_γ. The concepts of the intrinsic state formalism are reviewed in the context of the consistent Q framework and shown to imply vanishing $\beta\rightarrow g$ transitions, for any boson number, in the absence of K mixing effects. The O(6) limit obtained with the consistent Q formalism is shown to be a special case of the general limit. Finally, transition regions are discussed, particularly the SU(3)—O(6) case, in terms of "trajectories" in χ_Q between its limiting values. A number of qualitative parameter-free predictions for the evolution of energy or $E2$ branching ratios are thus obtained.

[NUCLEAR STRUCTURE Consistent Q formalism of the IBA. Energy and $B(E2)$ predictions, contour plots, χ_Q trajectories, intrinsic state formalism.]

I. INTRODUCTION

One of the distinguishing features of the interacting boson approximation[1] (IBA) is its ability to describe the changing collective properties of nuclei across an entire major shell within the framework of a single, simple Hamiltonian. This feature stems from the fact that the analogs of limiting geometrical descriptions (vibrational, rotational, γ unstable) appear naturally within the framework of the IBA Hamiltonian, in terms of the symmetries SU(5), SU(3), and O(6) associated with its group theoretical foundations. Thus, for example, both the vibration-rotation transition in the Sm and Gd nuclei[2,3] and the deformed-γ-unstable transition in the Os-Pt nuclei[4] have been reproduced with considerable success in the IBA-1 basis. In these earlier calculations, the three limiting symmetries of the model each corresponded to the dominance of a particular term in the Hamiltonian, and the transition between two symmetries was generated by adjusting the relative sizes of the appropriate terms. However, more recently, studies in the region of deformed nuclei have suggested a somewhat different approach.

Calculations in deformed nuclei require the use of a $Q\cdot Q$ interaction coupling the IBA basis states, where the boson quadrupole operator consists of two terms, of the form $(s^\dagger\tilde{d}+d^\dagger s)^{(2)}$ and $(d^\dagger\tilde{d})^{(2)}$. The appropriate limiting symmetry in this case is SU(3) which arises in the Hamiltonian when the two terms are in the specific ratio of $-\sqrt{7}/2$. In addition, the complete symmetry, incorporating transition rates, necessitates the use of the same ratio of terms in the quadrupole operator describing $E2$ transitions. The predicted energy spectrum in the limit involves degenerate β and γ bands, while the $E2$ selection rules forbid, for instance, transitions between γ and g bands. Since the first of these features is seldom realized in deformed nuclei, and the second never, the symmetry must be broken in realistic calculations.

In the earlier calculations the perturbation introduced in the Hamiltonian[5,6] was a $P\cdot P$ term which, when dominant, generates the O(6) symmetry. However, it has been shown in a recent study[6] that the breaking of the symmetry in the Hamiltonian alone is not sufficient to provide an adequate description of relative $B(E2)$ values. The reproduction of these latter data requires, in addition, the use of a very different ratio of terms in the quadrupole $E2$ operator than the SU(3) ratio. Thus, to date, the successful reproduction of the empirical properties in deformed nuclei has necessitated the use of different forms of the quadrupole operator in H and $T(E2)$.

While there is no reason *a priori* to assume that a multipole operator in a Hamiltonian should have the same parametrization as that used in the description of electromagnetic transitions, in many models such a relationship is frequently assumed in the case of the quadrupole

operator, particularly in deformed nuclei where it can be related to the equilibrium nuclear shape. In fact, in the IBA-2 framework,[7] where neutron and proton degrees of freedom are treated separately, this constraint has always been applied. Moreover, it has already been suggested[6] that, in the IBA-1 framework, the adoption of a similar constraint might obviate the need for an additional term in the Hamiltonian for deformed nuclei since the symmetry breaking induced by changing the parametrization of Q in the Hamiltonian, in the direction indicated by the empirically determined $E2$ operator, should be of a similar nature to that produced by the $P\cdot P$ term.

The current study, therefore, is aimed at investigating the utility of an IBA-1 formalism which uses a consistent parametrization of the quadrupole operator in both the Hamiltonian and $E2$ operators. Some of the principal results have already been briefly reported elsewhere.[8] It will be shown that this approach indeed produces the perturbation to the SU(3) symmetry required to reproduce the properties of deformed nuclei without, in many cases, the need for an additional symmetry breaking term. The new framework then involves one *less* free parameter than the earlier one but, as will be seen, provides equivalent or improved agreement with the data. The three limiting symmetries of the model can still be attained and, in fact, a description of the overall structural characteristics of the nuclei spanning the SU(3) and O(6) regions (e.g., Gd to Pt) can be attempted in terms of a *single* free parameter. An important consequence of this simplification is that effects stemming specifically from the changing boson number across this region are more easily identified, thus highlighting the importance of the inclusion of finite boson number in the IBA basis.

II. THE CONSISTENT Q FORMALISM

The Hamiltonian employed in the current approach is of the form

$$H=-\kappa Q\cdot Q-\kappa' L\cdot L\ , \tag{1}$$

with the quadrupole operator being specified as

$$Q=(s^{\dagger}\tilde{d}+d^{\dagger}s)^{(2)}+(\chi_Q/\sqrt{5})(d^{\dagger}\tilde{d})^{(2)} \tag{2}$$

so that the ratio of the two terms in the operator is defined by the parameter χ_Q. The calculation of $E2$ transition probabilities in the model involves the use of an operator

$$T(E2)=\alpha Q\ , \tag{3}$$

where α represents the boson effective charge.

As pointed out in the Introduction, the basis of the current approach is to employ a *variable* χ_Q in the Hamiltonian, but to demand *the same value* in the description of $E2$ transitions. The SU(3) limit of the model thus appears when $\chi_Q=-\sqrt{35}/2$ (so that the ratio of the two terms in Q is $-\sqrt{7}/2$) while, when $\chi_Q=0$, Q in Eq. (2) becomes a generator of O(6) and hence the formalism yields a specific form of the O(6) limit which, it will be seen, corresponds to that found empirically[9] in ^{196}Pt. The gross structural changes involved in the transition between SU(3) and O(6)-like structure can then be predicted simply as a function of χ_Q and the boson number N. This feature stems from the particularly simple structure of the Hamiltonian of Eq. (1). The $L\cdot L$ term is always diagonal, and therefore has no effect on the final wave functions. The IBA basis states are those of SU(5), and since no term in ϵn_d appears in the Hamiltonian, they are initially degenerate and are therefore mixed solely by the $Q\cdot Q$ interaction. The *relative* sizes of all the matrix elements are thus specified entirely by χ_Q, for a given boson number N. The parameter κ acts simply as a scaling factor, which determines the overall energy splitting of the states. In addition, the *relative* energies of states of the same spin will also depend only on χ_Q and N. Finally, since the $E2$ quadrupole operator is defined to be identical to that in H, its structure is also given by χ_Q, so that all relative $B(E2)$ values are uniquely determined by χ_Q and N. A single $B(E2)$ ratio can thus be used to determine χ_Q for a given nucleus, which then determines the wave functions, relative excitation energies, and all other $B(E2)$ values.

III. APPLICATION TO THE DEFORMED REGION

In determining the values of χ_Q appropriate to the region of well deformed nuclei, the most suitable empirical quantity is the ratio

$$B(E2;2_{\gamma}^{+}\rightarrow 0_{g}^{+})/B(E2;2_{g}^{+}\rightarrow 0_{g}^{+})\ ,$$

which is usually well known. This quantity is zero in both the rigorous SU(3) and O(6) limits of the IBA, and its variation in the intermediate regime can be studied in the form of a contour plot versus χ_Q and N, as shown in Fig. 1. The hatched area in the center of the plot corresponds to the empirical range of the $B(E2)$ ratio in the deformed region, where N varies between 12 and 16, and yields a range of χ_Q values of ≈ -0.9 to -1.4 for these nuclei. The fact that these values are not those of SU(3) (-2.958) reflects the fact, mentioned earlier, that $\gamma\rightarrow g$ transitions in well deformed nuclei are of collective strength whereas they vanish in the rigorous SU(3) limit. The narrow range of χ_Q values is a consequence of the remarkable stability of the γ mode throughout this region.

The fitted hatched region of Fig. 1 can now be transferred to other contour plots of $B(E2)$ ratios or energy ratios, and thus used to predict the properties of other excitations within this simple framework. This raises an important point, in that, in the IBA, the properties of all the intrinsic excitations are "coupled," in the sense that the gross characteristics of all are determined, in this formalism, by χ_Q and N. Thus, in particular, the properties of the low lying $K^{\pi}=0^{+}(\beta)$ mode in deformed nuclei are, in effect, determined by those of the γ mode, and can now be predicted. The appropriate contour plots are shown in Fig. 2. Note that the energy ratio plotted eliminates the rotational contribution to the γ band head energy, while the Clebsch-Gordan coefficients in both numerator and denominator of the $B(E2)$ ratio are identical in magnitude, so that the chosen ratios compare the properties of the *intrinsic* excitations in each case.

The hatched regions in Fig. 2 yield the prediction that, relative to the γ band, the $K^{\pi}=0^{+}$ mode should be 1.4—1.7 times higher in energy and have a $B(E2)$ strength

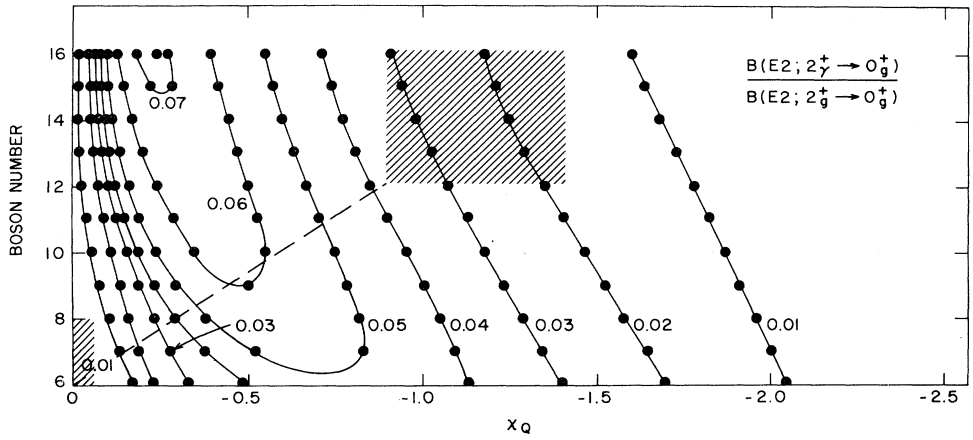

FIG. 1. Contour plot of the ratio $B(E2;2^+_\gamma \rightarrow 0^+_g)/B(E2;2^+_g \rightarrow 0^+_g)$. The hatched area in the center denotes the range of χ_Q and N values appropriate to well deformed nuclei, while that in the lower left corresponds to O(6) (Pt) nuclei. The dashed line represents a linear interpolation of χ_Q values between the two hatched regions. The 2^+_γ state has been taken as the second excited 2^+ state in all cases.

to the ground band 50—300 times weaker. Empirically these properties are at least qualitatively verified since the first 0^+ excitation is found at energies of 1—2 times that of the γ band in the majority of deformed nuclei, while the $B(E2)$ strength to the ground band is 10—100 times weaker. The empirical systematics of these quantities in deformed nuclei have been discussed in detail elsewhere.[6] As pointed out in these earlier studies, the weakness of the ground state $B(E2)$ branch can be contrasted with the geometrical concept of the β mode being a collective quadrupole excitation built on the ground state, with consequently enhanced $E2$ transitions between these two bands. A further essential characteristic of the β mode in the IBA is the prediction of collective $E2$ matrix elements to the γ band; the relevant contour plot is shown in Fig 3. Again, the range of χ_Q and N values appropriate to deformed nuclei is indicated by the hatched area, and it can be seen that the $\beta \rightarrow \gamma$ branch is expected to be of comparable strength to $\gamma \rightarrow g$ transitions, and thus to dominate the $\beta \rightarrow g$ branch. Again, this represents a notable departure from previous geometrical concepts, where $\beta \rightarrow \gamma$ transitions would only arise from band mixing effects. Empirically, there is little information available to date on these transitions, since the E^5_γ dependence of the overall transition rate greatly reduces the observed intensity of these low energy transitions. However, in three cases, ^{158}Gd, ^{166}Er, and ^{168}Er, data do exist[10–12] and imply values of

$$B(E2;2^+_\gamma \rightarrow 0^+_\beta)/B(E2;2^+_\gamma \rightarrow 0^+_g)$$

of unity or greater.

While the simple Hamiltonian of Eq. (1), with appropriate choice of χ_Q, represents a much improved starting point in an IBA description of a deformed nucleus, in general, it will be necessary to introduce additional terms to

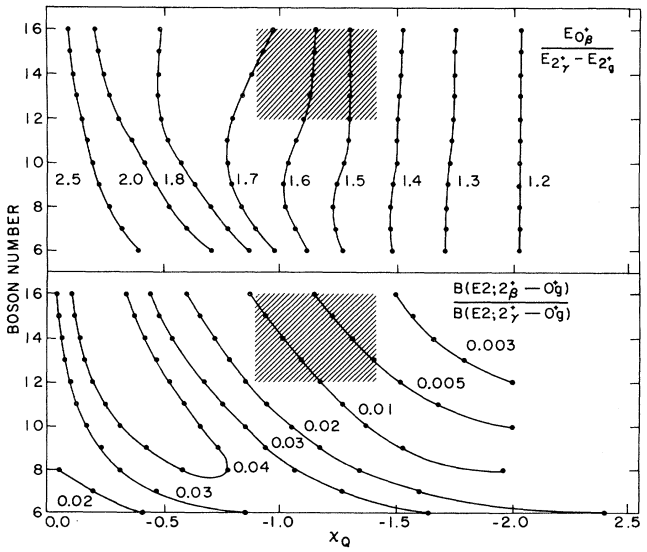

FIG. 2. Contour plot showing the relative predicted properties of the β and γ bands. The upper portion gives the ratio of intrinsic energies, and the lower the ratio of $B(E2)$ strengths to the ground band. The 0^+_β level has been taken as the first excited 0^+ state throughout, and the 2^+_β level is that which is connected to the 0^+_β level by a $B(E2)$ strength of enhanced magnitude. The hatched region in each case shows the χ_Q and N values for well deformed nuclei.

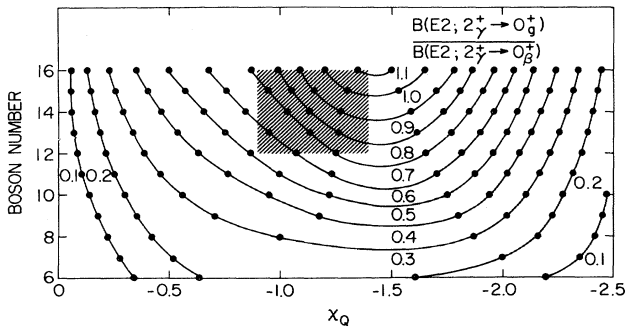

FIG. 3. Contour plot of the relative strengths of the $\gamma \rightarrow g$ and $\gamma \rightarrow \beta$ transitions. (See Figs. 1 and 2 for details.)

describe more accurately, for instance, the characteristics of the 0^+ band. The obvious choice for such a purpose is the $P\cdot P$ term, which has been shown[6] to affect the 0^+ band significantly, but to leave the properties of the ground and γ bands essentially unchanged. Nevertheless, the gross relative characteristics of the low lying excitations will remain the same. Moreover, in the case of ^{168}Er, for example, it has already been shown[8] that the simple treatment discussed here in fact results in improved agreement with the data, when compared to the earlier approach employing an SU(3) form of Q in the Hamiltonian as well as a $P\cdot P$ term, and using a different structure of Q in the $E2$ operator. This improvement is evident, for example, in the predicted $\gamma\rightarrow g$ transition strengths, which are compared in Table I, and is particularly impressive when it is recalled that the current calculation involves one *less* free parameter than the earlier one.

In considering the general properties of the γ band in the current framework, the energy and intrinsic $\gamma\rightarrow g$ $B(E2)$ strengths are used to determine the parameters κ and χ_Q, and hence cannot serve to test predictions of the model. However, a more subtle effect can be studied, namely, that of $\Delta K=2$ band mixing. In a geometrical framework, the relative strengths of all the $\gamma\rightarrow g$ transitions in a particular nucleus are simply given by the squares of the appropriate Clebsch-Gordan coefficients. Empirical deviations from these values, such as those shown in Table I, are usually ascribed to a mixing of the (geometrical) ground and γ excitations, and used to extract the degree of mixing, which is commonly described[13] by the parameter Z_γ. Aside from their absolute values, the empirical Z_γ values display an interesting systematics; they are large at the edge of the deformed region, and minimize at midshell. In the current framework, it might be hoped that such effects would automatically result from the chosen formalism, by virtue of its dependence on χ_Q and N. Figure 4 presents the empirical Z_γ values, plotted against N, and compares them with the IBA calculations.[14] It is evident that the empirical systematics are indeed well reproduced; in particular, the distinct dependence on boson number. Although there is also some dependence on the chosen χ_Q values, it has been demonstrated[14] that for the well deformed nuclei in Fig. 4, with $N=12-16$, the narrow spread in χ_Q values implies that the dominant origin of these systematics in the IBA framework is indeed the changing boson number. This feature has been dealt with in detail in a separate publication.[14]

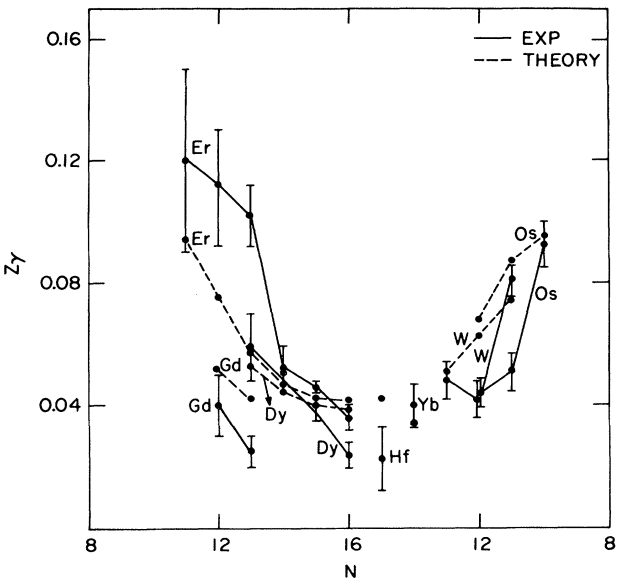

FIG. 4. Empirical and calculated Z_γ values as a function of boson number N, taken from Ref. 14. The points with error bars, joined by solid lines, are the data. The dashed lines connect the calculated values.

TABLE I. Relative $\gamma\rightarrow g$ $B(E2)$ values from the γ band in ^{168}Er.

I_i	I_f,K_f	Exp[a]	Alaga	IBA[b] $(P\cdot P)$	IBA[c] (χ_Q)
2	0,0	54	70	66	54
	2,0	100	100	100	100
	4,0	7	5	6	8
3	2,0	100	100	100	100
	4,0	65	40	48	69
4	2,0	20	34	30	18
	4,0	100	100	100	100
	6,0	14	9	12	16
5	4,0	81	175	72	80
	6,0	100	100	100	100
6	4,0	12	27	23	9
	6,0	100	100	100	100
	8,0	37	11	17	20

[a]Data from Ref. 11.
[b]IBA results from calculations of Ref. 5
[c]IBA results from calculations in current formalism, with $\chi_Q=-1.1$.

Given the narrow deduced range of χ_Q, which leads to a small predicted spread in many of the various empirical quantities, it is worthwhile to summarize this section by suggesting a "deformed limit" for the IBA, illustrated in the upper part of Fig. 5 and corresponding to "average" values of χ_Q and N of -1.1 and 14, respectively. As mentioned above, this limit actually corresponds very closely to the low lying structure of ^{168}Er, and some additional examples of nuclei close to this structure are shown in the lower portion of the figure. The energy scale denotes the relative energies of the low lying excitations, on a scale in which the γ band intrinsic energy is unity, since this quantity can be fixed by the parameter κ in Eq. (1). As mentioned earlier, the lack of any empirical information on the $\beta\rightarrow\gamma$ transitions in the cases shown, except for ^{168}Er, reflects the need for more sensitive spectroscopic studies, rather than the confirmed absence of such branches.

Although many other deformed nuclei may be amenable to a treatment incorporating a small additional $P\cdot P$ term in the Hamiltonian of Eq. (1), there are some notable exceptions, specifically, the Yb nuclei where, in ^{172,174}Yb for example, the γ band is well *above* the first excited 0^+ excitation. However, these nuclei show a number of other

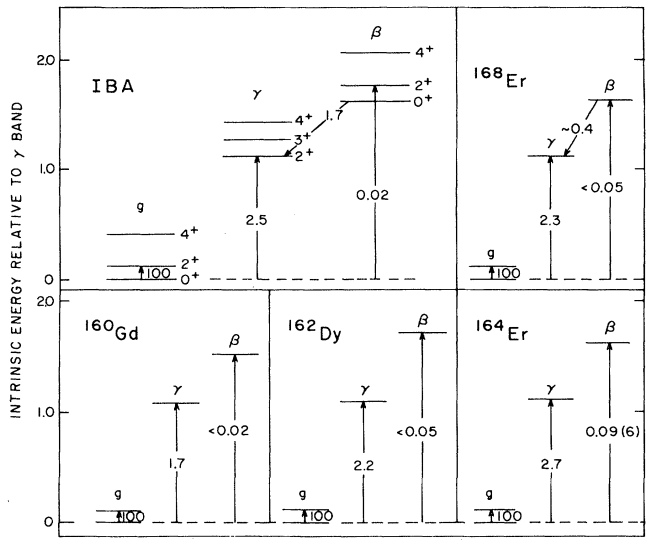

FIG. 5. The upper left shows the average predicted structure of a deformed nucleus in the current IBA formalism (see the text). The remainder shows four empirical examples which correspond closely to this prediction. The numbered arrows give the relative $B(E2)$ strengths between the bands. The data are from Refs. 12, 15–17.

features which suggest a significant difference in structure from their neighbors. The most obvious of these are the γ band energies themselves, which are 1466 and 1634 keV in ^{172}Yb and ^{174}Yb, respectively, compared to a "normal" range across the deformed region of $\approx$800–1200 keV. Moreover, the $\gamma \rightarrow g$ $B(E2)$ strength is about a factor of 2 lower than the other nuclei in this region.

IV. THE INTRINSIC STATE FORMALISM

It is by now evident that the IBA predicts properties of the first 0^+ excitation in deformed nuclei which differ substantially from those expected of a β vibration. These differences become particularly apparent if the intrinsic state formalism, introduced in Refs. 18–20, is used to simulate the Hamiltonian of Eq. (1). In this formalism, the IBA intrinsic ground state for an axially symmetric deformed nucleus, in the limit of pure K values, is written as

$$|g\rangle=(N!)^{-1/2}(b_c^\dagger)^N|0\rangle\ , \tag{4}$$

with

$$b_c^\dagger=(1+\beta^2)^{-1/2}(s^\dagger+\beta d_0^\dagger)\ . \tag{5}$$

The parameter β takes the value $\sqrt{2}$ in the pure SU(3) limit of the IBA, and can be related[18] to the corresponding deformation parameter in the geometrical framework by recalling that in the latter, the deformation applies to the total nuclear volume, while in the IBA, it applies only to the $2N$ valence nucleons. Thus we can expect that, very roughly,

$$\beta_{\rm geom}\approx(2N/A)\beta_{\rm IBA}\ . \tag{6}$$

The equilibrium value of β which corresponds to a given χ_Q and N value in the Hamiltonian can be obtained by minimizing, with respect to β, the expectation value of $Q\cdot Q$ in the ground state (4), thus yielding[18] a relationship between χ_Q and β, viz.

$$1-k\beta-\beta^2=0\ , \tag{7}$$

where $k=\sqrt{2/35}\chi_Q$. The intrinsic state of the first excited 0^+ band is obtained[20] by replacing one of the condensate bosons by the orthogonal combination of $s^\dagger$ and $d_0^\dagger$

$$|\beta\rangle=N^{-1/2}b_\beta^\dagger b_c|g\rangle\ , \tag{8}$$

where

$$b_\beta^\dagger=(1+\beta^2)^{-1/2}(-\beta s^\dagger+d_0^\dagger)\ . \tag{9}$$

The intrinsic matrix element of the $E2$ operator of Eq. (2), between β and g bands, is then given by[21]

$$\langle g|T_0(E2)|\beta\rangle=qN^{1/2}(1+\beta^2)^{-1}(1-k\beta-\beta^2)\ . \tag{10}$$

It is immediately evident that the function in χ_Q and β on the right of this equation is identical to that of Eq. (7) so that *the $\beta\rightarrow g$ transitions are predicted to be identically zero in this consistent Q framework, for any N.* Small, but nonzero $\beta\rightarrow g$ $B(E2)$ values are, however, seen empirically, and also result from numerical IBA calculations because the intrinsic state approach presented here neglects certain higher order effects included in the full IBA treatment. For instance, it assumes pure K values while the IBA automatically incorporates K mixing. The corresponding $\beta\rightarrow\gamma$ matrix element has been given in Ref. 21, and is nonzero under the condition (7). Thus the IBA β band, in this intrinsic state approximation, is seen to be characterized by enhanced transitions to the γ band and zero strength to the ground band, the exact inverse of the pattern of decay expected from a "pure" β vibration. Moreover, while it has become widely accepted that the IBA and Bohr-Mottelson Hamiltonians become equivalent when the former is taken to the limit of infinite N, the result described above would seem to indicate that this equivalence does not hold for all $E2$ matrix elements. Hopefully, this feature may prove useful in establishing a geometrical counterpart to the IBA β band.

V. THE O(6) LIMIT

As pointed out in the Introduction, when χ_Q is taken as zero, the quadrupole operator in H becomes a generator of O(6) and hence a level scheme with O(6) symmetry results. The predicted properties of such a symmetry have been found[9] to correspond closely to the empirical situation in ^{196}Pt, and are described in detail in Refs. 4 and 9. However, in this earlier study, the symmetry was generated by the use of terms in $P\cdot P$ and $L\cdot L$, as well as an "octupole" term $[\approx(d^\dagger\tilde{d})^{(3)}]$. The resulting eigenvalue expression was given by

$$E=(\tfrac{1}{4})A(N-\sigma)(N+\sigma+4)+B\tau(\tau+3)+CL(L+1)\ , \tag{11}$$

where A, B, and C are constants related to the strengths of the three interactions employed. In the current study, only two interactions are used, namely, $Q\cdot Q$ (with $\chi_Q \equiv 0$) and $L\cdot L$, and the corresponding eigenvalue expression necessarily contains only two constants, i.e.,

$$E = A'[(N+\sigma)(N+\sigma+4)+\tau(\tau+3)]+C'L(L+1)\,, \tag{12}$$

where $A'=2\kappa$ and $C'=-\kappa'$. Thus the current approach represents a special case of the earlier one, in which $A/4\equiv B$. Remarkably, in the earlier study,[9] the parameters deduced for ^{196}Pt were $A=185$ keV and $B=42$ keV, and thus very close to the required 4:1 ratio. The current formalism will therefore produce equivalent agreement, in terms of both energy and $B(E2)$ data, for ^{196}Pt, and it will be interesting to see whether future empirical examples of the O(6) symmetry correspond to the specific form of Eq. (12). Moreover, recent work[22] in the IBA-2 basis shows that it is possible to generate the O(6) symmetry in that framework also, and, interestingly, the eigenvalue expression which emerges is again that of Eq. (12).

VI. THE SU(3)—O(6) TRANSITION

It is now evident that the transition in structure between the O(6) limit in ^{196}Pt and the well deformed region can be represented by varying χ_Q between its corresponding values of 0 and ~ -1.1. The simplest assumption of a linear interpolation between these two regions would correspond to the dashed line on the contour plot of Fig. 1. In fact, as shown in Fig. 6, the actual behavior of the χ_Q values, deduced from $B(E2)$ ratios, for the nuclei in this transitional region is remarkably close to this simple dependence. Note that the sign of the quadrupole moment of the 2_1^+ state depends on the sign of χ_Q, and hence small positive χ_Q values have been ascribed to the Pt nuclei, to reflect the negative quadrupole moments observed empirically. Also, the range of χ_Q values for the majority of deformed nuclei is seen to be even narrower than suggested originally, from -0.9 to -1.2, the extension to larger absolute values being necessary only for the Gd nuclei. Thus, an inescapable prediction of Fig. 1 is that the plotted $B(E2)$ ratio should *peak* in going from the O(6) limit to deformed nuclei, and this prediction is compared with the data in Fig. 7. It can be seen that this ratio indeed

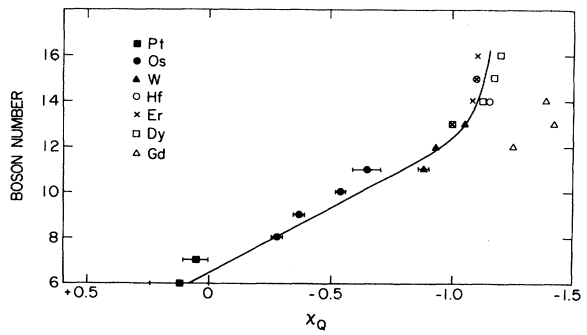

FIG. 6. Values of χ_Q, extracted from $B(E2)$ ratios, for nuclei in the Gd-Pt region.

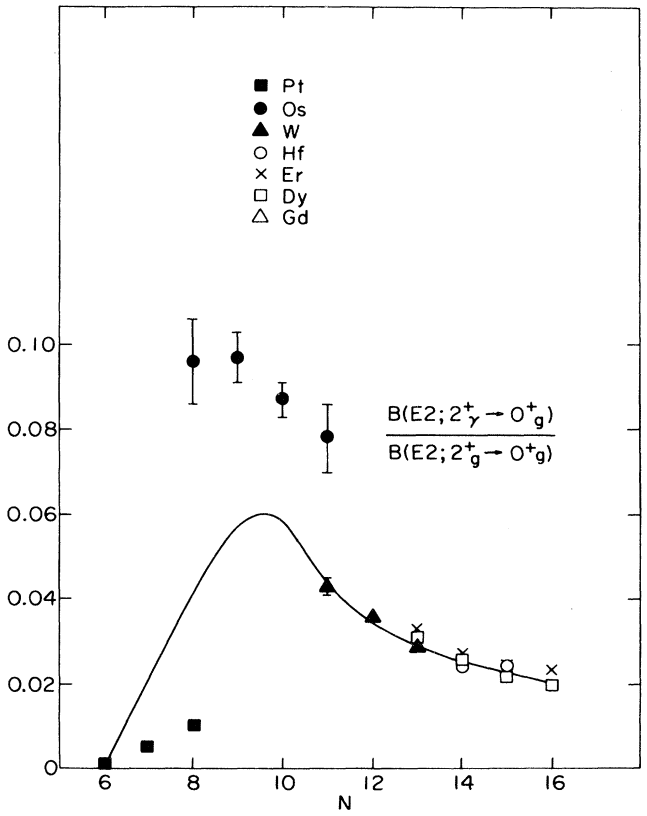

FIG. 7. Empirical behavior of the $B(E2)$ ratio of Fig. 1 compared with the IBA calculations (solid line) resulting from the use of χ_Q values taken from the dashed line of Fig. 1. The data are from Refs. 23—28.

maximizes in the Os nuclei, although the empirical values are larger than can be obtained from the simple Hamiltonian adopted, indicating the need for additional term(s) to obtain more precise agreement. Also, the simple assumed behavior of χ_Q vs N is not adequate for the Pt nuclei which appear to require $\chi_Q$values which change more slowly.

The behavior of other quantities in this transitional region can, of course, be predicted in a similar manner, and two additional examples are shown in Fig. 8. On the right-hand side of Fig. 8, the *branching* ratio from the 2_γ^+ state is plotted, and it is evident that there is no peaking predicted in this case, and that the data again follow the calculated trend. Note that in the deformed region, the curve is asymptotically approaching the rotational (Alaga) values of 0.7 for this ratio, but does *not* attain it. This feature reflects the "automatic" incorporation of band mixing effects in the IBA Hamiltonian. On the left-hand side of Fig. 8, the predictions for the quadrupole moments of the first 2^+ states are shown and compared with the data. In this case, since the prediction involves an *absolute* $E2$ matrix element, a value must be chosen for the effective charge α, and the curves corresponding to two such values, 0.14 and 0.125 e b, are shown. Since, effectively, all the data falls within these two curves, it can be inferred that the effective charge is close to a constant throughout

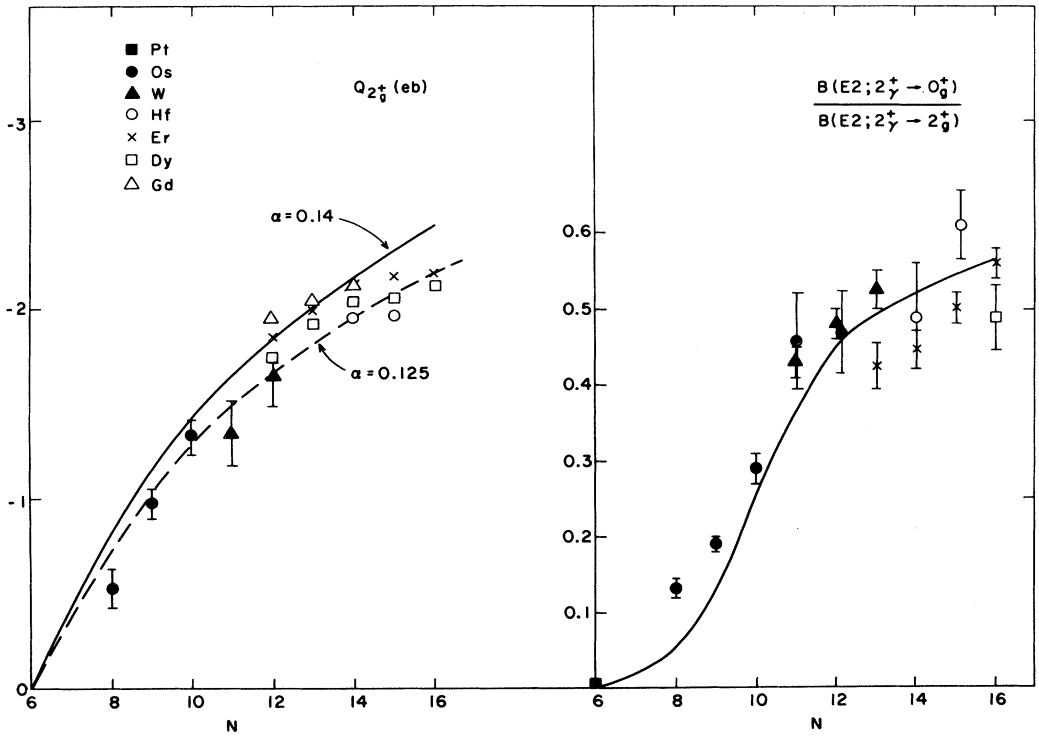

FIG. 8. Comparison of the empirical and predicted trends in (left-hand side) the quadrupole moments of the 2_1^+ state and (right-hand side) the $B(E2)$ branching ratio from the second excited 2^+ state across the deformed-O(6) region. The data are from Refs. 23, 28—33. The calculated trend is shown by the solid or dashed lines in each case. On the left-hand side, two calculated curves have been drawn, corresponding to the two different values of the boson effective charge shown.

the O(6)—SU(3) region. Nevertheless, two other features which may indicate the need for small changes in this quantity are evident. First, while the data for the deformed region clearly exhibit an N dependence, the slope of Q vs N suggests that α itself may have a small N dependence. In addition, the empirical Q values seem to separate according to Z indicating, not unreasonably, the need for a slightly different effective charge for each element.

VII. THE SU(5)—SU(3) TRANSITION

In the previous discussions, both the SU(3) and O(6) limits could be generated by choosing a specific value of χ_Q in the quadrupole operator, and nuclei exhibiting structure close to, or between, these limits could be described in terms of the changing structure of Q. However, in considering the transition towards SU(5) (vibrational) structure, the utility of this formalism is not clear.

The rigorous SU(5) limit in the IBA is generated by a term of the form ϵn_d, where ϵ is the boson energy, and involves *no* contribution from the $Q\cdot Q$ interaction. In the transitional nuclei between deformed and SU(5) regions, both terms will be necessary, and the unique and simple dependence of the wave functions and $B(E2)$ values on χ_Q and N will therefore be lost. Moreover, the question arises as to the structure of Q applicable to this region, since the SU(5) limit provides no indication in this respect. Calculations[2,3] using the SU(3) form of Q in the Hamiltonian provide good agreement with data for the transitional Sm and Gd nuclei, but require the use of a different quadrupole operator for $E2$ transitions. On the other hand, the use of a consistent Q approach, with the value of χ_Q appropriate to deformed nuclei, does *not* allow the empirical $B(E2)$ values to be reproduced.

The likely behavior of χ_Q in this region can be deduced by considering the relationship of this formalism to the IBA-2 Hamiltonian. In the latter framework, neutron and proton degrees of freedom are treated separately, and the parameters of the Hamiltonian can, in principle, be related to the underlying shell structure. Moreover, the neutron proton interaction employed is of the form $Q_\pi\cdot Q_\nu$, where Q_π and Q_ν have the form of Eq. (2) and are parametrized by χ_π and χ_ν. It is possible to project the IBA-2 parameters into the IBA-1 basis, and this procedure yields the simple relationship

$$\chi_Q=(\chi_\pi+\chi_\nu)/2\ .$$

The expected behavior of χ_π and χ_ν is such that both take the large negative values appropriate to SU(3) at the beginning of their respective shells and become progressively more positive in going across the shell. Thus, χ_Q can be expected to approach its *SU(3)* value of -2.958 during the transition to *SU(5)* structure. Indeed, as pointed out in Sec. VI, there is already some indication of this tendency in the heavier Gd nuclei.

VIII. SUMMARY AND CONCLUSIONS

It has been shown that the use of a consistent quadrupole operator in H and $T(E2)$ in the IBA-1 formalism provides a simple framework which allows the major structural characteristics of the deformed-O(6) region to be described in terms of a single free parameter, and the boson number. It has been emphasized that this approach may not be adequate to obtain detailed agreement with experiment in all cases, so that additional terms of the original Hamiltonian may have to be reintroduced as, presumably, smaller perturbations in any specific calculation. Nevertheless, in certain cases, such as ^{168}Er, the consistent Q formalism may provide improved agreement with the data without any such additional terms. This improvement, resulting from a *reduction* in the number of free parameters, gives a clear indication that this approach represents a preferable starting point, at least for IBA-1 calculations in this region.

The simplicity of the formalism allows the majority of observable properties to be predicted, rather than fitted. In the deformed region, the most crucial predictions center on the decay modes of the β band, which were shown to be the inverse of those expected of a geometrical β vibration. The empirical evidence clearly favors the IBA interpretation, and the intriguing question thus remains as to the geometrical interpretation of the IBA β band. The application of the intrinsic state formalism to this problem further emphasizes the difference in the two descriptions and shows that, in the consistent Q framework employed here, the IBA $\beta \rightarrow g$ $E2$ matrix element is identically zero for any N. This result would indicate that the major differences in the predicted decay of the β mode stem from *differences in the specific operators* employed in the two models. In fact, a recent study[34] suggests that, if the volume conservation condition is taken to second order in the liquid drop model, instead of to first order as has been done in the past, the available operators in the geometrical framework become identical to those in the IBA. It remains to be ascertained how this modification affects the $K=0$ and 2 vibrational modes in the former model, and why the latter is so much less affected than the former.

The overall characteristics of the transition to the O(6) limit have been shown to be well reproduced as a function of χ_Q and N. Moreover, in the preceding section, it was pointed out that χ_Q can be obtained from the equivalent parameters in the IBA-2 basis via the projection technique, and thus, in principle, from the underlying microscopic description. This feature has some important consequences. It implies that the values of χ_Q obtained in the current study provide constraints on the values of χ_π and χ_ν which must be derived from the shell model basis. In particular, the narrow range of χ_Q determined for the deformed region implies an equivalent restriction on the sign and magnitude of $(\chi_\pi+\chi_\nu)$. Moreover, it is clear from the current study that an eventual theoretical determination of the behavior of χ_π and χ_ν will allow the structure of the nuclei spanning the deformed-O(6) region to be predicted without *any* parametrization. Thus the crucial features arising from an IBA-1 calculation, which is normally regarded as essentially a phenomenological approach, can in fact be predicted from the underlying shell model basis. It is, of course, the explicit inclusion of the finite valence nucleon number in the IBA basis which permits such a connection to be made.

ACKNOWLEDGMENTS

The authors would like to thank O. Scholten for providing the coding changes necessary to implement the revised Hamiltonian. They are also grateful to F. Iachello, P. von Brentano, A. Faessler, R. Bijker, A. E. L. Dieperink, D. H. Feng, R. Gilmore, M. Vallieres, and J. Wood for useful discussions, and to H. Dejbakhsh and A. Aprahamian for help with some of the numerical calculations. This research was performed under Contract No. DE-AC02-76CH00016 with the United States Department of Energy.

[1]A. Arima and F. Iachello, Ann. Phys. (N.Y.) 99, 253 (1976); 111, 201 (1978); 123, 468 (1979).

[2]O. Scholten, F. Iachello, and A. Arima, Ann. Phys. (N.Y.) 115, 325 (1978).

[3]P. Van Isacker, R. Heyde, M. Waroquier, and G. Wenes, Nucl. Phys. A380, 383 (1982).

[4]R. F. Casten and J. A. Cizewski, Nucl. Phys. A309, 477 (1978).

[5]D. D. Warner, R. F. Casten, and W. F. Davidson, Phys. Rev. C 24, 1713 (1981).

[6]D. D. Warner and R. F. Casten, Phys. Rev. C 25, 2019 (1982).

[7]T. Otsuka, A. Arima, F. Iachello, and I. Talmi, Phys. Lett. 76B, 139 (1978); T. Otsuka, A. Arima, and F. Iachello, Nucl. Phys. A309, 1 (1978).

[8]D. D. Warner and R. F. Casten, Phys. Rev. Lett. 48, 1385 (1982).

[9]J. A. Cizewski, R. F. Casten, G. J. Smith, M. R. Macphail, M. L. Stelts, W. R. Kane, H. G. Borner, and W. F. Davison, Nucl. Phys. A323, 349 (1979).

[10]R. C. Greenwood, C. W. Reich, N. A. Baader, M. R. Koch, D. Breitig, O. W. B. Schult, B. Fogelberg, A. Backlin, W. Mampe, T. von Egidy, and K. Schreckenbach, Nucl. Phys. A304, 327 (1978).

[11]F. K. McGowan, Phys. Rev. C 24, 1803 (1981).

[12]W. F. Davidson, D. D. Warner, R. F. Casten, K. Schreckenbach, H. G. Borner, J. Simic, M. Stojanovic, M. Bogdanovic, S. Koicki, W. Gelletly, G. B. Orr, and M. L. Stelts, J. Phys. G 7, 455 (1981); 7, 843 (1981).

[13]L. L. Riedinger, N. R. Johnson, and J. H. Hamilton, Phys. Rev. 179, 1214 (1969).

[14]R. F. Casten, D. D. Warner, and A. Aprahamian, Phys. Rev. C (to be published).

[15]F. K. McGowan and W. T. Milner, Phys. Rev. C 23, 1926 (1981).

[16]R. M. Ronningen, J. H. Hamilton, L. Varnell, J. Lange, A. V. Ramayya, G. Garcia-Bermudez, W. Laurens, L. L. Riedinger, F. K. McGowan, P. H. Stelson, R. L. Robinson, and J. L. C. Ford, Jr., Phys. Rev. C 16, 2208 (1977).

[17]R. M. Ronningen, R. J. Grantham, J. H. Hamilton, R. B. Piercey, A. V. Ramayya, B. van Noijen, W. K. Dagenhart, L. L. Riedinger, H. Kawakami, C. S. Maguire, and R. S. Lee, Oak

Ridge National Laboratory Annual Progress Report, 1976.
[18]J. N. Ginnochio and M. W. Kirson, Nucl. Phys, A350, 31 (1980).
[19]A. E. L. Dieperink, O. Scholten, and F. Iachello, Phys. Rev. 44, 1742 (1980).
[20]A. E. L. Dieperink and O. Scholten, Nucl. Phys. A346, 125 (1980); A. Bohr and B. R. Mottelson, Phys. Scr. 25, 28 (1982).
[21]R. Bijker and A. E. L. Dieperink, Phys. Rev. C 26, 2688 (1982).
[22]A. E. L. Dieperink, *Progress in Particle and Nuclear Physics, Collective Bands in Nuclei,* edited by Sir Denys Wilkinson (Pergamon, New York, 1983), Vol. 9, p. 121.
[23]C. Baktash, J. X. Saladin, J. J. O'Brien, and J. G. Alessi, Phys. Rev. C 22, 2383 (1980).
[24]F. K. McGowan, W. T. Milner, R. L. Robinson, and P.H. Stelson, Nucl. Phys. A297, 51 (1978).
[25]R. M. Ronningen, J. H. Hamilton, A. V. Ramayya, L. Varnell, G. Garcia-Bermudez, J. Lange, W. Lourens, L. L. Riedinger, R. L. Robinson, P. H. Stelson, and J. L. C. Ford, Jr., Phys. Rev. C 15, 1671 (1977).
[26]M. J. Martin and P. H. Stelson, Nucl. Data Sheets 21, 1 (1977).
[27]J. K. Tuli, Nucl. Data Sheets 12, 477 (1974).
[28]W. T. Milner, F. K. McGowan, R. L. Robinson, P. H. Stelson, and R. O. Sayer, Nucl. Phys. A177, 1 (1971).
[29]A. Christy and O. Hausser, Nucl. Data Tables 11, 281 (1973).
[30]S. C. Guyrathi and J. M. D'Auria, Nucl. Phys. A172, 353 (1971).
[31]A. Buyrn, Nucl. Data Sheets 14, 471 (1975).
[32]J. M. Domingos, G. D. Symons, A. C. Douglas, Nucl. Phys. A180, 600 (1972).
[33]F. W. N. DeBoer, P. T. A. Goudsmit, P. Koldewijn, and B. J. Meijer, Nucl. Phys. A169, 577 (1971).
[34]R. Gilmore and D. H.Feng, Phys. Lett. 125B, 99 (1983).